International Journal of Rotating Machinery
2001, Vol. 7, No. 5, pp. 323–333
Reprints available directly from the publisher
Photocopying permitted by license only

Stabilization of Centrifuges with Instabilities Due to Fluid–Structure Interactions: Various Control Approaches

HEINZ ULBRICH*, ADRIAN CYLLIK and GUIDO AHAUS

Universität-GH Essen, Lehrstuhl für Mechanik, FB 12, Schützenbahn 70, 45127 Essen, Germany

(Received 30 May 2000; In final form 21 June 2000)

Partially filled centrifuges exhibit unstable behavior over particular rotational speed ranges. To remove this unstable behavior, three different control approaches are presented which are experimentally implemented using a magnetic bearing. First, by means of a PD-controller the system stiffness is changed leading to a shift of the instability region. Second, the instability region is removed by a cross coupled feed back of the rotor vibration velocities. This cross coupling directly counteracts the fluid excitation mechanism. Third, a disturbance observer is presented which allows to estimate and compensate the not exactly known fluid force.

Keywords: Centrifuge; Viscous fluid model; Control approaches; Magnetic bearing

1. INTRODUCTION

In industry partially filled centrifuges are used in different fields, *e.g.*, as sugar- or dirty-water-centrifuges or separators for the separation of fluids with different densities. In certain rotational speed ranges couplings between the motion of the rotor and the motion of the rotating fluid lead to an unstable behavior of the centrifuge. Since passive measures do not offer any or only unsatisfying solutions and do not allow to change the system parameters in operation, the objective of the present research is to actively remove the instability using a magnetic bearing.

For the design of suitable approaches for stabilizing the fluid-rotor-system a model was presented in (Ulbrich *et al.*, 1990; Ulbrich *et al.*, 1998 and Ahaus, 1999). In (Ulbrich *et al.*, 1996) the fluid viscosity was neglected leading to an unstable behavior in the simulation over the whole operating range when external damping was considered. This discrepancy to the experimental results is eliminated when the fluid viscosity is taken into account (Ulbrich *et al.*, 1998; Ahaus,

*Corresponding author. Tel.: 49-201-183-2905, Fax: 49-201-183-2871, e-mail: ulbrich@uni-essen.de

1999). Besides these research works, the viscous fluid model was investigated by (Hachmann, 1989; Riedel, 1992) and others. Although the non-viscous and viscous models yield similar results, the viscous fluid model renders a more exact stability statement. However, the disadvantage of the viscous fluid model is that the equation of motion can not be described in the time domain (Ahaus, 1999). Based on these models the three control approaches described in this paper are designed and experimentally verified on a test rig.

Control approaches for the stabilization of a partially filled centrifuge have been presented by (Takagi *et al.*, 1993 and Matsushita *et al.*, 1988). Takagi used a PD-controller which allows to shift the instability region to another speed range. He determined two different pairs of PD-values for two non-overlapping instability regions of a centrifuge modeled as a rigid body and supported by two active magnetic bearings. By switching between these two different PD-values the system remains stable throughout the considered speed range. Matsushita removed the instability by damping a specific forward natural motion that he identified as the unstable natural motion of the system. He achieved this by a cross coupled feedback of the rotor deflection. Because he needed only the components of the deflection signal related to the unstable natural motion, these components have been determined by a tuning filter that was manually adjusted to the respective rotational speed.

The first control concept presented in this paper, the PD-controller, is based upon the approach presented by Takagi. The PD-controller is applied to the present test rig and its effect is illustrated with respect to design parameters.

The second control approach, the velocity cross coupling, is derived from investigating the excitation mechanism of the instability. As the induced fluid force is proportional to the rotor vibration velocity and acts perpendicular to it, the system can be stabilized by a cross coupled velocity feedback.

In the third concept the fluid force is regarded as a disturbance force which is estimated by a disturbance observer and compensated by the active magnetic bearing.

2. MODEL DESCRIPTION

In the model of the investigated centrifuge the fluid container is mounted on top of the vertical shaft. The shaft is supported by a fixed bearing at the bottom and by an elastically mounted bearing in the middle of the shaft (see Fig. 1). Because of the low stiffness of the upper bearing (compared with the rotor stiffness), at first the rotor was considered as a rigid body.

During the verification process it became evident that the magnetic bearing excites not only the rigid body eigenmode, but also the first two bending eigenmodes of the shaft. Therefore, the rotor model presented in (Ulbrich *et al.*, 1996 and Ulbrich *et al.*, 1998) is extended using the FE-program MADYN. Introducing the control vector $\mathbf{u}=[u_x, u_y]^T$ and the vector of fluid effects $\mathbf{f}_F=[F_{Fx}, F_{Fy}, M_{Fx}, M_{Fy}]^T$ the equations of motion are given by

$$\tilde{\mathbf{M}}\ddot{\tilde{\mathbf{q}}} + (\boldsymbol{\Omega}\tilde{\mathbf{G}} + \tilde{\mathbf{D}})\dot{\tilde{\mathbf{q}}} + \tilde{\mathbf{K}}\tilde{\mathbf{q}} = \tilde{\mathbf{J}}_M\mathbf{u} + \tilde{\mathbf{J}}_F\mathbf{f}_F \quad (1)$$

where $\tilde{\mathbf{q}}$ is the vector of the position coordinates. Using the modal matrix $\boldsymbol{\Phi}$, where

$$\boldsymbol{\Phi}^T\tilde{\mathbf{M}}\boldsymbol{\Phi} = \mathbf{I}, \quad (2)$$

and considering only the first three eigenmodes both for the *xz*- and for the *yz*-plane, Eq. (1) is reduced to

$$\ddot{\mathbf{q}} + (\boldsymbol{\Omega}\mathbf{G} + \mathbf{D})\dot{\mathbf{q}} + \mathbf{K}\mathbf{q} = \mathbf{J}_M\mathbf{u} + \mathbf{J}_F\mathbf{f}_F. \quad (3)$$

The vector $\mathbf{q}$ contains the six modal coordinates (three for each plane), the vectors $\mathbf{u}$ and $\mathbf{f}_F$ account for the control forces and fluid effects. The three eigenmodes included in the reduced model are depicted in Figure 1.

For the magnetic force in x-direction, f_{Mx}, the following linear relationship is assumed:

$$f_{Mx} = k_s x + k_i i. \quad (4)$$

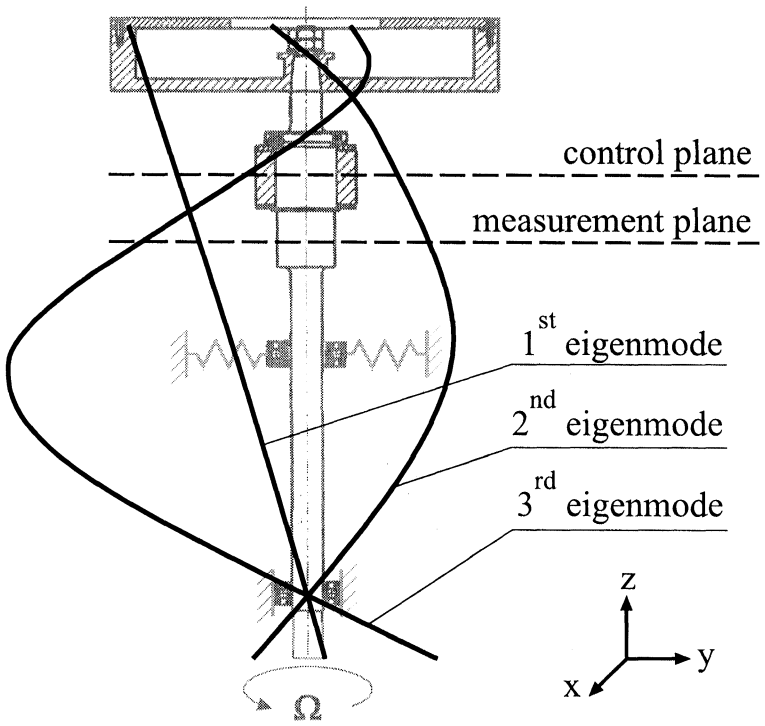

FIGURE 1 Sketch of the centrifuge and its relevant eigenmodes.

The same applies to the y-direction. In Eq. (3), the negative stiffness k_s and the control current i are already accounted in the stiffness-matrix $\mathbf{K}$ and in the control vector $\mathbf{u}$, respectively.

The vector of the fluid effects is described depending on the modal position vector

$$\mathbf{f}_F = \mathbf{F}\mathbf{J}_F^T\mathbf{q}, \tag{5}$$

where $\mathbf{F}$ represents the viscous fluid model and shall not be described in more detail here because of its complex structure. A detailed derivation is given in (Ahaus, 1999). It should be remarked that this matrix shows the following dependence on the eigenvalues λ of Eq. (3):

$$\mathbf{F} = \mathbf{F}\left(\sqrt{\lambda_i}, \lambda_i, \lambda_i^2, \dots\right). \tag{6}$$

Additionally, $\mathbf{F}$ depends on other parameters like the rotational speed $\mathbf{\Omega}$, the viscosity ν of the fluid and the filling ratio f, which is the quotient of the radius b of the free liquid surface and the inner radius a of the casing ($f = b/a$). As the fluid matrix $\mathbf{F}$ contains square roots of the eigenvalues, Eq. (3) can not be evaluated in the time domain, but only in the frequency domain. With the formulation

$$\mathbf{q} = \bar{\mathbf{q}}e^{\lambda t}, \tag{7}$$

substituting Eqs. (5) and (7) into Eq. (3) yields

$$(\mathbf{I}\lambda_i^2 + (\mathbf{\Omega G} + \mathbf{D})\lambda_i + \mathbf{K} - \mathbf{J}_F\mathbf{F}\mathbf{J}_F^T)\bar{\mathbf{q}}_i = \mathbf{0}. \tag{8}$$

In this case, Eq. (8) describes the homogeneous system. This equation can be extended by the control vector $\mathbf{u}$ as shown in Eq. (12). The eigenvalues of Eqs. (8) or (12) are numerically determined using standard optimization methods (*e.g.*, the Levenberg- or Gauss–Newton-method).

As already mentioned, the influence of the control vector $\mathbf{u}$ on the modal position vector $\mathbf{q}$ is determined by the input matrix $\mathbf{J}_M$. On the other

hand, the output matrix $\mathbf{J}_{\text{sen}}$ transforms the modal coordinates into physical coordinates:

$$\begin{bmatrix} x \\ y \end{bmatrix} = \mathbf{y} = \mathbf{J}_{\text{sen}}\mathbf{q}. \tag{9}$$

The matrices $\mathbf{J}_M$ and $\mathbf{J}_{\text{sen}}$ are calibrated such that the voltages in $\mathbf{y}$ are proportional to the rotor deflections and the voltages in $\mathbf{u}$ are proportional to the control currents. The position of the control and measurement plane is represented in Figure 1. The control and measurement unit can be described as an ideal proportional feed back element in the considered frequency range.

3. TEST RIG

The test rig was already presented in (Ulbrich *et al.*, 1996 and Ulbrich *et al.*, 1998). Here, only the essential features are listed:

- The upper roller bearing's stiffness is adjustable.
- The rotational speed range extends from 0 to 50 Hz.
- The rotor deflections in x- and y-direction are measured contact-free with two eddy current sensors.
- The control forces affect the centrifuge contact-free and are induced by an active magnetic bearing (max. force 350 N, nominal air gap 0.8 mm).
- The uncontrolled (passive) test rig has an unstable region for rotor frequencies from 7 to 13 Hz (Ulbrich *et al.*, 1998).

4. CONTROL APPROACHES

4.1. PD-controller

The PD-controller is implemented analogously to Takagi's concept. Like in Takagi's case, the PD-controller controls the magnetic bearing (compensation of the negative stiffness k_s) and relocates the instability region. The resulting control vector $\mathbf{u}$ is

$$\mathbf{u} = \mathbf{u}_{\text{PD}} = -\mathbf{R}_{\text{P}}\mathbf{J}_{\text{sen}}\mathbf{q} - \mathbf{R}_{\text{D}}\mathbf{J}_{\text{sen}}\dot{\mathbf{q}} \tag{10}$$

with

$$\mathbf{R}_{\text{P}} = \begin{bmatrix} p & 0 \\ 0 & p \end{bmatrix} \quad \text{and} \quad \mathbf{R}_{\text{D}} = \begin{bmatrix} d & 0 \\ 0 & d \end{bmatrix}. \tag{11}$$

Using Eqs. (10), (3) and (7), Eq. (8) can be extended to

$$\begin{aligned}(\mathbf{I}\lambda_i^2 + (\Omega\mathbf{G} + \mathbf{D})\lambda_i + \mathbf{K} - \mathbf{J}_F\mathbf{F}\mathbf{J}_F^T \\ + \mathbf{J}_M\mathbf{R}_{\text{P}}\mathbf{J}_{\text{sen}} + \mathbf{J}_M\mathbf{R}_{\text{D}}\mathbf{J}_{\text{sen}}\lambda_i)\bar{\mathbf{q}}_i = \mathbf{0}.\end{aligned} \tag{12}$$

According to Eq. (12), p could be determined such that the instability region lies above the one of the passive system. The quasi-stationary startup behavior of both systems is represented in Figure 2. Two non-overlapping instability regions exist whereby the upper instability region's boundary of the PD-controlled system lies outside of the realizable speed range of the test rig. The amplitudes of this upper boundary of the PD-controlled system illustrated in Figure 2 are estimated. When the PD-controller is turned on during the startup just before the instability region of the passive system is reached, the instability region is shifted and the startup is readily carried out. If the passive system's unstable region is passed the PD-controller is switched off in order to stay out of the instability region of the PD-controlled system.

Analogously to the behavior of the PD-controlled system, the position of the instability region of the passive system depends on the upper roller bearing's stiffness and thus on the system stiffness. When increasing the system stiffness, the instability region is shifted to higher rotational speeds and extends over a greater speed range (see Fig. 3 – the boundary lines are not closed for $1-f^2=0$ and $1-f^2=1$ because the model does not apply to an empty or totally filled container). As the system stiffness can be influenced by the PD-controller, too, one can move the instability region in an equivalent way either by changing the stiffness of the upper bearing or by changing the P-gain.

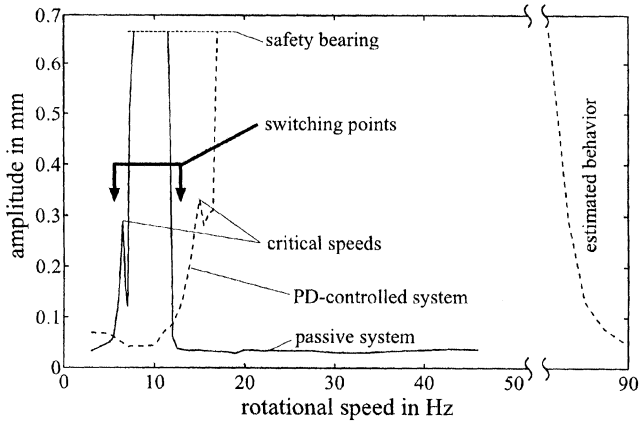

FIGURE 2 Startup behavior of the passive and the PD-controlled system ($p = 1.4$, $d = 0.0015$ s).

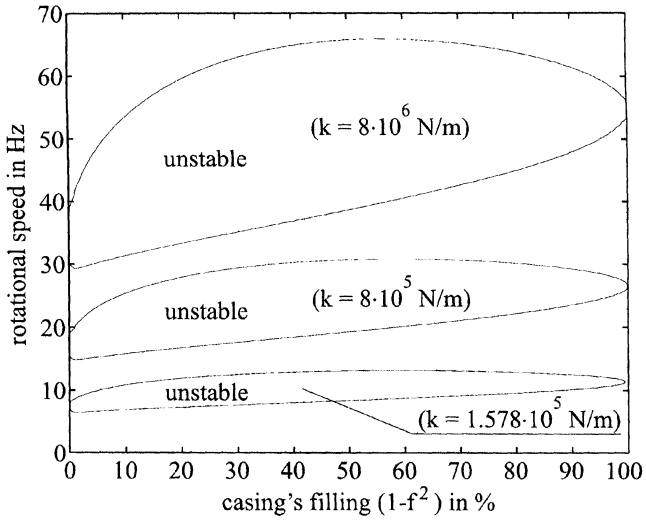

FIGURE 3 Instability region of the passive system depending on the stiffness k of the upper roller bearing.

If the design parameters of a centrifuge are known, the instability region could be positioned by a suitable choice of the system stiffness such that it lied above the operating speed range, thus providing stability in the entire speed range. To that end, however, the plant might have to be designed very stiff. In this case the operating speed would be below the instability region, but the plant would have to be operated subcritically, which led to higher vibration amplitudes and thus to a higher load in the plant. Hence, the advantage of the active magnetic bearing is that the system stiffness can be varied as desired (restricted by the saturation of the control force). Thus, the instability region can be passed and the plant can be operated supercritically.

4.2. Velocity Cross Coupling

The drawback of the PD-controller is that the instability region might not be shifted high enough for certain system configurations so that

the instability region of the uncontrolled and controlled system overlap. In this case, other control approaches are needed to stabilize the centrifuge.

An alternative control concept is derived from the characteristics of those fluid force components that lead to an excitation of the rotor vibrations. For that purpose, a partially liquid-filled container rotating with $\boldsymbol{\Omega} = \text{const.}$ around its axis is considered which is excited harmonically along its x-axis and y-axis, respectively (no DOFs). Considering the phase of the vibration-exciting components of the transfer function matrix $\mathbf{f}_F/\bar{\mathbf{q}}$ that account for the vibration excitation, the characteristics shown in Figure 4 are obtained. The phases jump to $-90°$ and $+90°$, respectively, in a wide range of the excitation frequency; the corresponding fluid force components are shown in Figure 5. The following relationships are obtained for this range:

$$F_{Fx} \sim \dot{y}_F, \quad F_{Fy} \sim \dot{x}_F, \tag{13}$$

where F_{Fx}, F_{Fy} are the fluid forces and $\dot{x}_F$, $\dot{y}_F$ are the velocities of the center of mass of the fluid container in x- respectively in y-direction.

In order to counteract the vibration-exciting fluid force components, a velocity cross coupling control law is derived:

$$\begin{aligned} \mathbf{u}_G &= -\begin{bmatrix} 0 & g(\boldsymbol{\Omega},f) \\ -g(\boldsymbol{\Omega},f) & 0 \end{bmatrix} \mathbf{J}_{\text{sen}}\dot{\mathbf{q}} \\ &= -\mathbf{R}_G\mathbf{J}_{\text{sen}}\dot{\mathbf{q}} \end{aligned} \tag{14}$$

The coupling factor g depends on $\boldsymbol{\Omega}$ and f and is determined as to provide stability for the particular operating point. To that end, the coupling factor g is increased until the real part of the unstable eigenvalue becomes negative and a sufficient stability reserve is obtained. Hence, only one coupling factor is sufficient for larger ranges of the rotational speed and the filling ratio.

In the continuous case, the cross-coupling factor can be increased without loosing stability until saturation of the control unit is reached. As the control is implemented on a digital controller

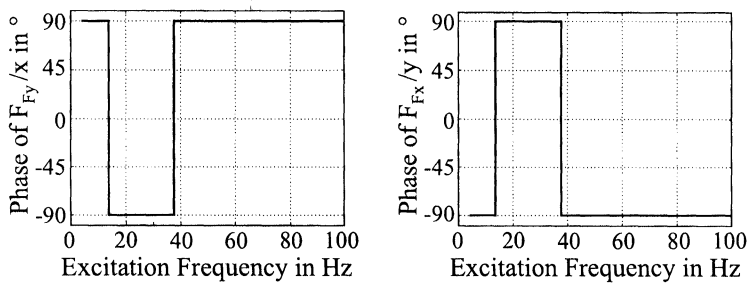

FIGURE 4 Phase frequency characteristics for a lateral harmonic excitation of the casing.

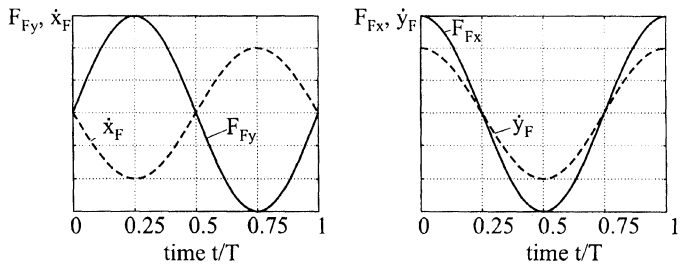

FIGURE 5 Vibration velocity and the resulting fluid force for a lateral harmonic excitation of the casing.

board, the system might turn unstable for high coupling factors due to *e.g.*, truncation effects or a time delay in the system. This effect holds for any filling ratio (for an empty container, too: comp. Ahrens, 1996) and was also verified on the test rig. By varying the feed back factor d the transition to the unstable behavior can be influenced. For the rotor without fluid, Figure 6 shows the boundary of the instability region in the discrete case as a function of the damping parameter d and the coupling factor g for a rotational speed $\Omega/2\pi = 12.8$ Hz.

Hence, for the choice of the coupling factor, both of the destabilizing effects (fluid excitation and truncation effects) have to be taken into consideration.

The effectiveness of the velocity cross coupling is represented in Figure 7 by a time plot of the x-deflection for a representative operating point ($g = 0.0025$ s, $\Omega/2\pi = 12.8$ Hz and $f = 0.894$, corresponding to a filling of the casing of 20%). Until $t = 3$ s the rotor deflection increases exponentially. The pulsing of the amplitude (beat) is caused by the superposition of two oscillations: The rotor motion corresponding to the rotational speed and the destabilizing natural motion of the fluid whose frequency is slightly lower than the rotor speed frequency (comp. Ulbrich *et al.*, 1998 and Fig. 8). Once the controller is switched on, the system is stabilized. The deflection is reduced and the pulsing of the amplitude decreases, *i.e.*, the fluid excitation is compensated.

The velocity cross coupling is a robust control approach, which directly counteracts the fluid forces. Similar to the PD-controller, only one coupling factor suffices for stabilizing large ranges of rotational speeds and filling ratios.

4.3. Disturbance Observer

The disturbance observer provides another possibility for the stabilization of the centrifuge. The basic idea consists in regarding the influence of the fluid as a disturbance which is not exactly known, but which can be observed based upon a simple model and then be compensated.

This system can be described using state space representation of Eq. (3):

$$\dot{\mathbf{x}} = \mathbf{A}\mathbf{x} + \mathbf{B}\mathbf{u} + \mathbf{B}_F\mathbf{z},$$

$$\mathbf{y} = \mathbf{C}\mathbf{x}, \tag{15}$$

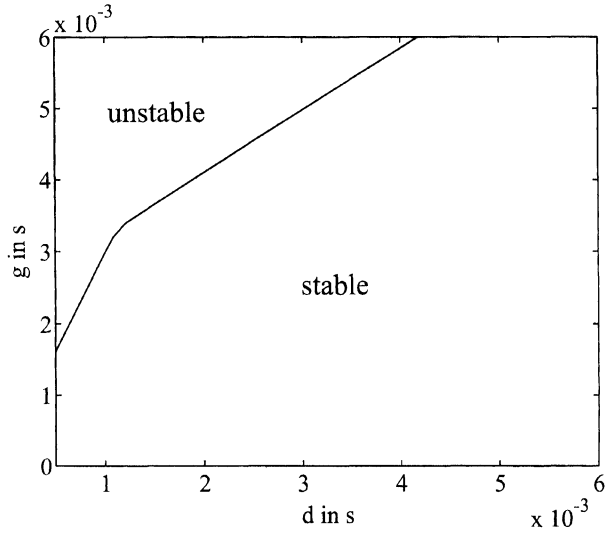

FIGURE 6 Instability region by use of digital velocity cross-coupling, depending on g and d ($\Omega/2\pi = 12.8$ Hz).

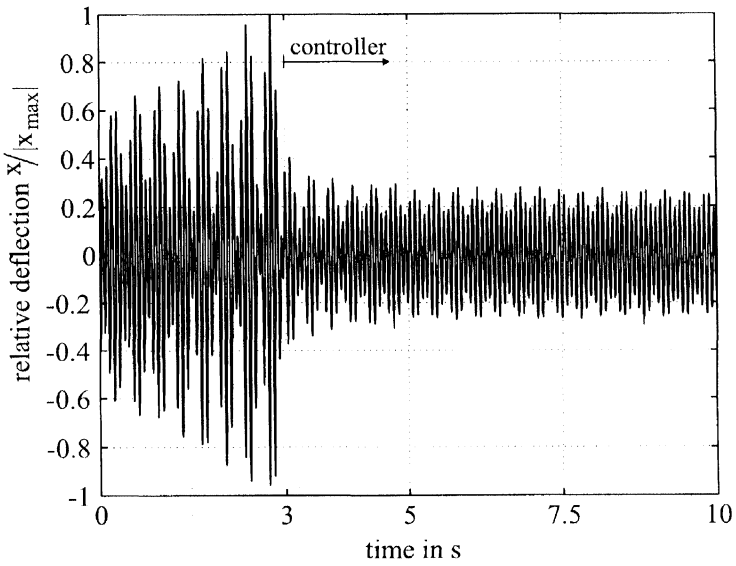

FIGURE 7 Measurement of the x-deflection: Effect of the velocity cross-coupling ($g = 0.0025\,\mathrm{s}$, $\boldsymbol{\Omega}/2\pi = 12.8\,\mathrm{Hz}$, $1 - f^2 = 20\%$).

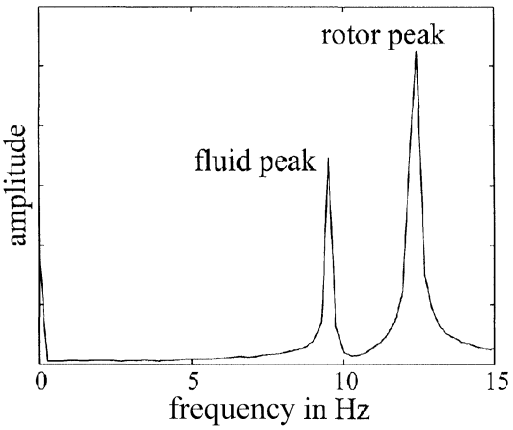

FIGURE 8 FFT of the deflection signal of the unstable system.

with

$$\mathbf{A} = \begin{bmatrix} \mathbf{0} & \mathbf{I} \\ -\mathbf{K} & -(\boldsymbol{\Omega}\mathbf{G} + \mathbf{D}) \end{bmatrix},$$

$$\mathbf{B} = \begin{bmatrix} \mathbf{0} \\ \mathbf{J}_M \end{bmatrix}, \quad \mathbf{B}_F = \begin{bmatrix} \mathbf{0} \\ \mathbf{J}_F \end{bmatrix},$$

$$\mathbf{x} = \begin{bmatrix} \mathbf{q} \\ \dot{\mathbf{q}} \end{bmatrix}, \quad \mathbf{C} = [\mathbf{J}_{\text{sen}} \quad \mathbf{0}] \quad \text{and} \quad \mathbf{z} = \begin{bmatrix} z_x \\ z_y \end{bmatrix}.$$

For observing the disturbance vector $\mathbf{z}$, a disturbance model is developed which describes the significant features of the disturbance. One characteristic feature is the "fluid frequency" corresponding to the unstable natural motion of the fluid (see Fig. 8).

The fluid frequency can be determined from Eq. (8) and depends on the filling ratio f and the rotor speed $\boldsymbol{\Omega}$. For a certain operating point, the following simplified fluid model is introduced

$$\ddot{\mathbf{z}} + \underbrace{\begin{bmatrix} 2\delta_F & 0 \\ 0 & 2\delta_F \end{bmatrix}}_{\mathbf{D}_F} \dot{\mathbf{z}} + \underbrace{\begin{bmatrix} \omega_F^2 & 0 \\ 0 & \omega_F^2 \end{bmatrix}}_{\mathbf{K}_F} \mathbf{z} = \mathbf{0}, \qquad (16)$$

where ω_F is the characteristic fluid frequency and δ_F is suitably chosen in order to obtain a robust system behavior of the disturbance observer when implementing it on the test rig.

Transforming Eq. (16) into state space representation

$$\begin{bmatrix} \dot{\mathbf{z}} \\ \ddot{\mathbf{z}} \end{bmatrix} = \begin{bmatrix} \mathbf{0} & \mathbf{E} \\ -\mathbf{K}_F & -\mathbf{D}_F \end{bmatrix} \begin{bmatrix} \mathbf{z} \\ \dot{\mathbf{z}} \end{bmatrix} \Leftrightarrow \dot{\mathbf{x}}_{\text{dis}} = \mathbf{A}_{\text{dis}}\mathbf{x}_{\text{dis}},$$

$$\mathbf{z} = [\mathbf{I} \quad \mathbf{0}]\mathbf{x}_{\text{dis}} \Leftrightarrow \mathbf{z} = \mathbf{C}_{\text{dis}}\mathbf{x}_{\text{dis}} \qquad (17)$$

and combining Eqs. (15) and (17) yields the extended model (index e):

$$\begin{bmatrix} \dot{\mathbf{x}} \\ \dot{\mathbf{x}}_{\text{dis}} \end{bmatrix} = \begin{bmatrix} \mathbf{A} & \mathbf{B}_F\mathbf{C}_{\text{dis}} \\ \mathbf{0} & \mathbf{A}_{\text{dis}} \end{bmatrix} \begin{bmatrix} \mathbf{x} \\ \mathbf{x}_{\text{dis}} \end{bmatrix} + \begin{bmatrix} \mathbf{B} \\ \mathbf{0} \end{bmatrix} \mathbf{u}$$

$$\Leftrightarrow \dot{\mathbf{x}}_e = \mathbf{A}_e\mathbf{x}_e + \mathbf{B}_e\mathbf{u},$$

$$\mathbf{y} = [\mathbf{C} \quad \mathbf{0}] \begin{bmatrix} \mathbf{x} \\ \mathbf{x}_{\text{dis}} \end{bmatrix} \Leftrightarrow \mathbf{y} = \mathbf{C}_e\mathbf{x}_e, \tag{18}$$

The observer is designed using the differential equation (Föllinger, 1992)

$$\dot{\hat{\mathbf{x}}}_e = (\mathbf{A}_e - \mathbf{L}_e\mathbf{C}_e)\hat{\mathbf{x}}_e + \mathbf{B}_e\mathbf{u} + \mathbf{L}_e\mathbf{y}, \tag{19}$$

where $\hat{\mathbf{x}}_e$ is the estimated state vector and $\mathbf{L}_e$ is the observer matrix which is determined by pole placement. The pole radii of the observer poles are chosen slightly greater than the pole radii of the plant. However, the real parts of the observer poles are smaller than those one of the plant poles. Thus, the observer is more damped than the plant.

To compensate the observed disturbance $\hat{\mathbf{x}}_{\text{dis}}$, an additional control voltage $\mathbf{u}_{\text{dis}}$ has to be determined and applied to the plant such that according to Eq. (15) the following condition has to be fulfilled:

$$\mathbf{B}\mathbf{u}_{\text{dis}} + \mathbf{B}_F\mathbf{C}_{\text{dis}}\hat{\mathbf{x}}_{\text{dis}} = \varepsilon \to \mathbf{0}. \tag{20}$$

Multiplying the left hand side with the pseudo inverse $\mathbf{B}^+$ leads to

$$\mathbf{u}_{\text{dis}} = -\mathbf{B}^+\mathbf{B}_F\mathbf{C}_{\text{dis}}\hat{\mathbf{x}}_{\text{dis}}, \tag{21}$$

which requires the control matrix $\mathbf{B}$ to have full rank.

Using Eq. (21), the disturbance compensation $\mathbf{u}_{\text{dis}}$ contains not only frequency components of the fluid frequency, but also components different from the fluid frequency. Therefore, $\mathbf{u}_{\text{dis}}$ as calculated in Eq. (21) is filtered with a band-pass filter (2nd order Butterworth).

The effect of the disturbance compensation can be seen from Figure 9 which shows the x-deflection for the same representative point of the instability region as in Section 4.2. The increasing deflection is stopped by switching on the disturbance observer in a similar way as by the use of the velocity cross coupling. The deflection is reduced and the fluid excitation removed.

With respect to the other two approaches, the disadvantage of this controller is that for every operating point (Ω,f) another observer model is

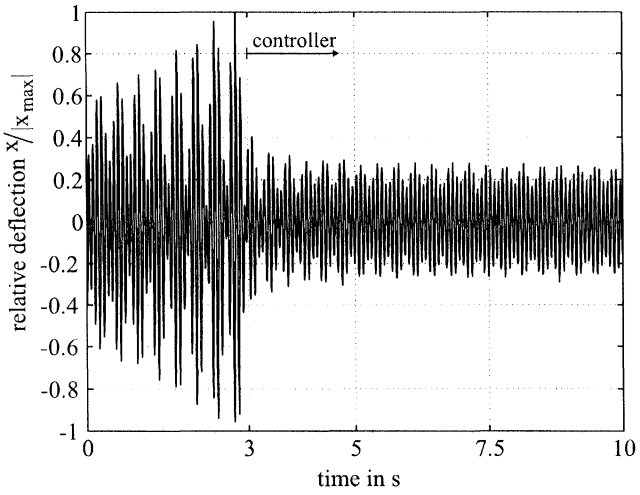

FIGURE 9 Measurement of the x-deflection: Effect of the disturbance compensation ($\Omega/2\pi = 12.8$ Hz, $1 - f^2 = 20\%$).

needed and that not only the deflection, but also the filling ratio f and the rotor speed $\mathbf{\Omega}$ have to be measured in order to determine the current operating point.

5. CONCLUSIONS

For removing the unstable behavior of a partially filled centrifuge, three control approaches are presented in this paper.

First, by means of the PD-controller, the instability region is shifted such that by appropriate switching between different PD-gains, the unstable region can be passed through during the startup. The advantage of this approach consists in obtaining a stable behavior of the centrifuge, regardless of the filling ratio and the rotational speed. The disadvantage is that the instability region might possibly not be shifted to sufficiently high rotor speeds due to the saturation of the control force.

Second, a velocity cross coupled feed back is proposed which stabilizes the centrifuge by directly counteracting the fluid force. For a wide range of the instability region only one coupling factor g is required so that the controller depends on the filling ratio and the rotational speed only to a small degree. Due to truncation effects, the coupling factor can not be chosen arbitrarily high. Therefore, the design has to be carried out with respect to both, the cross coupling g and the velocity feed back factor d, which suppresses the destabilization effects caused by truncation.

As for the last control approach, a disturbance observer is presented. The fluid force which does not have to be known exactly is represented by a simplified model. After designing a suitable observer, the fluid force can be estimated and compensated. The disadvantage of this approach is that for every operating point a new disturbance model is required and that not only the deflection, but also the filling ratio and the rotational speed have to be measured in order to determine the current operating point.

NOMENCLATURE

a	inner radius of the casing in m
b	inner radius of the free liquid surface in m
d	velocity feed back factor in s
f	filling ratio
f_M	magnetic bearing's force in N
g	velocity coupling factor in s
k_i	force-current-factor in N/A
k_s	negative bearing stiffness in N/m
p	deflection feed back factor
x_F, y_F	displacements of the fluid container in x-respectively in y-direction
$\dot{x}_F$, $\dot{y}_F$	velocities of the fluid container in x-respectively in y-direction
λ	eigenvalue
$\mathbf{\Omega}$	rotational speed in 1/s
$\mathbf{f}_F$	vector of the fluid effects
$\tilde{\mathbf{q}}$	vector of position coordinates
$\mathbf{q}$	reduced modal vector of position coordinates
$\mathbf{u}$	control vector
$\mathbf{x}$	state vector
$\mathbf{x}_e$	state vector of the extended model
$\mathbf{z}$	disturbance vector
ω_F	characteristic fluid frequency in 1/s
ζ_F	damping ratio of the fluid motion in 1/s
$\mathbf{A}$	state matrix
$\mathbf{A}_{\text{dis}}$	state matrix of the disturbance model
$\mathbf{A}_e$	state matrix of the extended model
$\mathbf{B}$	control matrix
$\mathbf{B}_F$	disturbance input matrix
$\mathbf{B}_e$	control matrix of the extended model
$\mathbf{C}$	output matrix
$\mathbf{C}_{\text{dis}}$	measurement matrix of the disturbance model
$\mathbf{C}_e$	output matrix of the extended model
$\tilde{\mathbf{D}}$	damping matrix
$\mathbf{D}$	reduced modal damping matrix
$\mathbf{F}$	matrix representing the viscous fluid model
$\tilde{\mathbf{G}}$	gyroscopic matrix
$\mathbf{G}$	reduced modal gyroscopic matrix
$\tilde{\mathbf{J}}_F$	input matrix of the fluid effects

$\mathbf{J}_F$	reduced modal input matrix of the fluid effects
$\tilde{\mathbf{J}}_M$	input matrix of the magnetic bearing's force
$\mathbf{J}_M$	reduced modal input matrix of the magnetic bearing's force
$\mathbf{J}_{\text{sen}}$	reduced modal output matrix
$\tilde{\mathbf{K}}$	stiffness matrix
$\mathbf{K}$	reduced modal stiffness matrix
$\mathbf{L}_e$	observer matrix of the extended model
$\tilde{\mathbf{M}}$	mass matrix
$\mathbf{R}_{\text{D}}$	velocity feed back matrix
$\mathbf{R}_G$	feed back matrix of the coupling factor
$\mathbf{R}_{\text{P}}$	deflection feed back matrix
$\mathbf{\Phi}$	modal matrix

References

Ahaus, G. (1999) Dynamik und regelungstechnische Stabilisierung einer elastischen, teilweise flüssigkeitsgefüllten Zentrifuge (Dynamics and Active Control Stabilization of an Elastic Centrifuge Partially Filled with Liquid), *Thesis*, Universität-GH Essen, Germany (in German).

Ahrens, M. (1996) Zur magnetischen Lagerung von Schwungrad-Energiespeichern (Magnetic Suspension for a Flywheel Energy Storage Device), *Thesis*, ETH No. 11930, Zurich, Switzerland (in German).

Föllinger, O. (1992) Control Theory (Regelungstechnik), 7th Edition, Hüthig-Verlag, Heidelberg, Germany (in German).

Hachmann, U. (1989) Viskose Dämpfung bei flüssigkeitsgeflülten Kreiseln (Viscous Damping of Liquid-Filled Gyroscopes), VDI-Fortschrittsberichte, Reihe 11: Schwingungstechnik, Nr. 118, VDI-Verlag, Düsseldorf, Germany (in German).

Matsushita, O., Takagi, M., Yoneyama, M., Saitoh, I., Nagata, A. and Aizawa, M. (1988) Stabilization by Cross Stiffness Control of Electromagnetic Damper for Contained Liquid Rotor Unstable Vibration, *Proc. IMechE 4th International Conference on Vibrations in Rotating Machinery*, Heriot-Wall, September 13–15, Paper No. C320/88, pp. 77–85.

Riedel, U. (1992) Laufstabilität flüssigkeitsgefüllter Zentrifugen (Stability of Liquid-Filled Centrifuges), VDI-Fortschrittsberichte, Reihe 11: Schwingungstechnik, Nr. 174, VDI-Verlag, Düsseldorf, Germany (in German).

Takagi, T., Tani, J., Zhang, H. and Murai, M. (1993) Experiment on Vibration Control of Viscous Liquid-Filled Rotor System Supported by Gain-Scheduled Active Magnetic Bearings, *Proceedings of the JSME, International Conference on Advanced Mechatronics*, Tokyo, pp. 34–37.

Ulbrich, H., Ahaus, G. and Cyllik, A. (1996) Stabilization of Elastic Rotors with Fluid Components on Magnetic Bearings, *Proceedings of the 5th International Symposium on Magnetic Bearings*, August, Kanazawa, Japan, pp. 31–36.

Ulbrich, H., Ahaus, G., Cyllik, A. and Zhu, C. (1998) Active Removal of Hydrodynamic Instabilities in Partially Filled Centrifuges, *Proceedings of the 7th International Symposium of Transport Phenomena and Dynamics of Rotating Machinery*, February 22–26, Honolulu, Hawaii, pp. 20–29.